V & Millstone Hill

Comparison of Arecibo vector neutral wind products in the F-region with ICON MIGHTI data in 2020

R.B. Kerr[1], S. Kapali[1], P.T. dos Santos[2], C.G.M. Brum[2], B. Harding[3]

[1]Computational Physics Inc. (CPI)
[2]University of Central Florida (UCF), Arecibo Observatory
[3]University of California, Berkeley

The Optical Laboratory at Arecibo Observatory. (AO). AO is managed and operated by the University of Central Florida in cooperative agreement with the National Science Foundation (NSF).
The Millstone Hill Optical Laboratory is supported by the NSF in agreement with the Massachusetts Institute of Technology and Haystack Observstory.

CEDAR 2021 Workshop
June 20-25, 2021

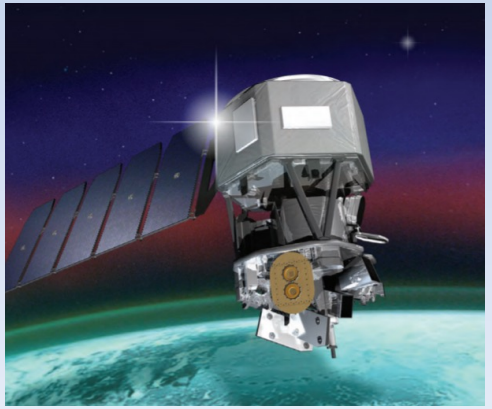

Credit: NASA ICON press kit, October, 2020. https://www.nasa.gov/sites/default/files/atoms/files/icon_presskit_oct2019.pdf.

The Instruments

The Arecibo Observatory (AO) Red Line Fabry-Perot Interferometer (FPI)

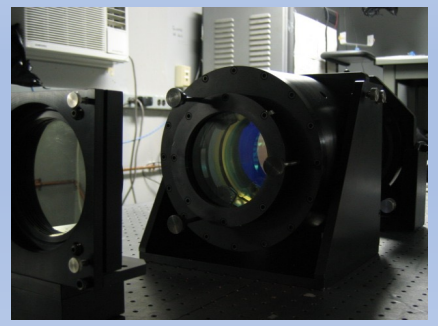

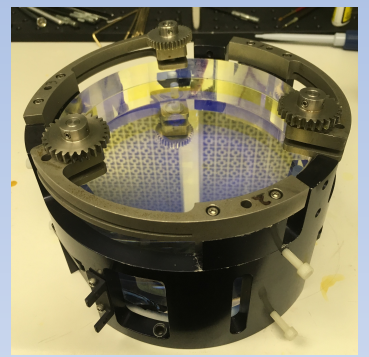

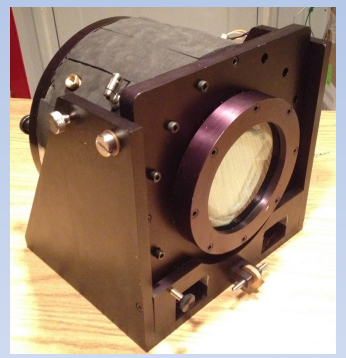

- A 150mm clear aperture Fabry-Perot interferometer
- An imaging instrument.
- Operational since 2012.

The Millstone Hill FPI is similar

- Operational since 2009
- 128 mm clear aperture

Michelson Interferometer for Global High-resolution Thermospheric Imaging (MIGHTI) (2 instruments)

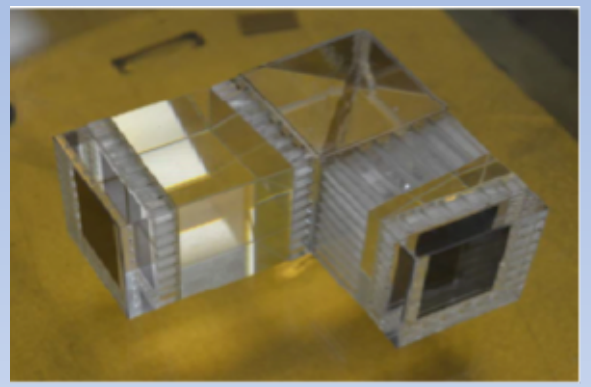

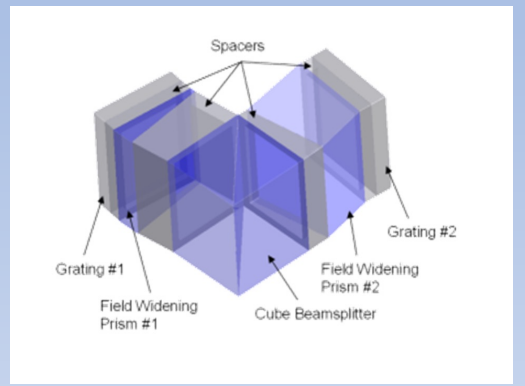

Credit: https://icon.ssl.berkeley.edu/Instruments/MIGHTI

- MIGHTI is a spatial heterodyne variant of a Michelson interferometer.
- MIGHTI uses a solid-state interferometer
- Heritage: WINDII (Wind Imaging Interferometer) UARS satellite [*Shepherd et al*., 1993]; SHIMMER (Spatial Heterodyne Imager for Mesospheric Radicals) STPSat-1 [*Englert et al*., 2008, 2010a, 2012]. REDDI (Redline DASH Demonstration Instrument) [*Harlander et al*., 2003, 2010]

The data

AO & MH FPIs

- ~2° field-of view (fov),
- Five-position beam swinging mirror system (N,S,E,W,Z) beneath a plexiglass dome
- Meridional and zonal wind vectors are derived from line-of-site (LOS) measurements of the 6300Å emission in the cardinal directions.
- Vectors assume a F2-region peak [e^-] at 250 km, & and peak volume emission altitude of 210 km.
- 1.5m – 3.0m CCD exposures in each direction
- Data are available from the “Madrigal” upper atmospheric science database: http://cedar.openmadrigal.org/
-

ICON MIGHTI

- Data used here are ICON data product 2.2, version level 4.0.
- fov = 3.2° (horiz. motion during exposure ~ 450 km)
- Meridional & zonal wind vectors are derived from LOS samples oriented 45° and 135° from the ICON velocity vector
- Velocity vector data and volume emission data are reported at 16 discrete altitudes in the thermosphere, from 160.3 km – 310.5 km.
- Data is available from: ftp://icon-science.ssl.berkeley.edu/pub/

The Comparison Filters

- All data from the 2020 calendar year
- ICON data correspond to nighttime hours at AO and MH (LST = 1800 – 0600)
- ICON measurement coordinates within a box ± 5° X ± 5° latitude and longitude centered on AO & MH
- Selected ICON data all carry data quality code = 1
- Selected ICON wind vectors correspond to the altitude of brightest 6300Å volume emission

With 3 data selection variations:

- ICON measurement coordinates within a box ± 5° X ± 5° latitude and longitude centered on AO & MH with AO/MH vector errors < 5 m/s
- ICON measurement coordinates within a box ± 2.5° X ± 2.5° latitude and longitude centered on AO/MH
- ICON measurement coordinates within a box ± 2.5° X ±2. 5° latitude and longitude centered on AO/MH with AO/MH vector errors < 5 m/s

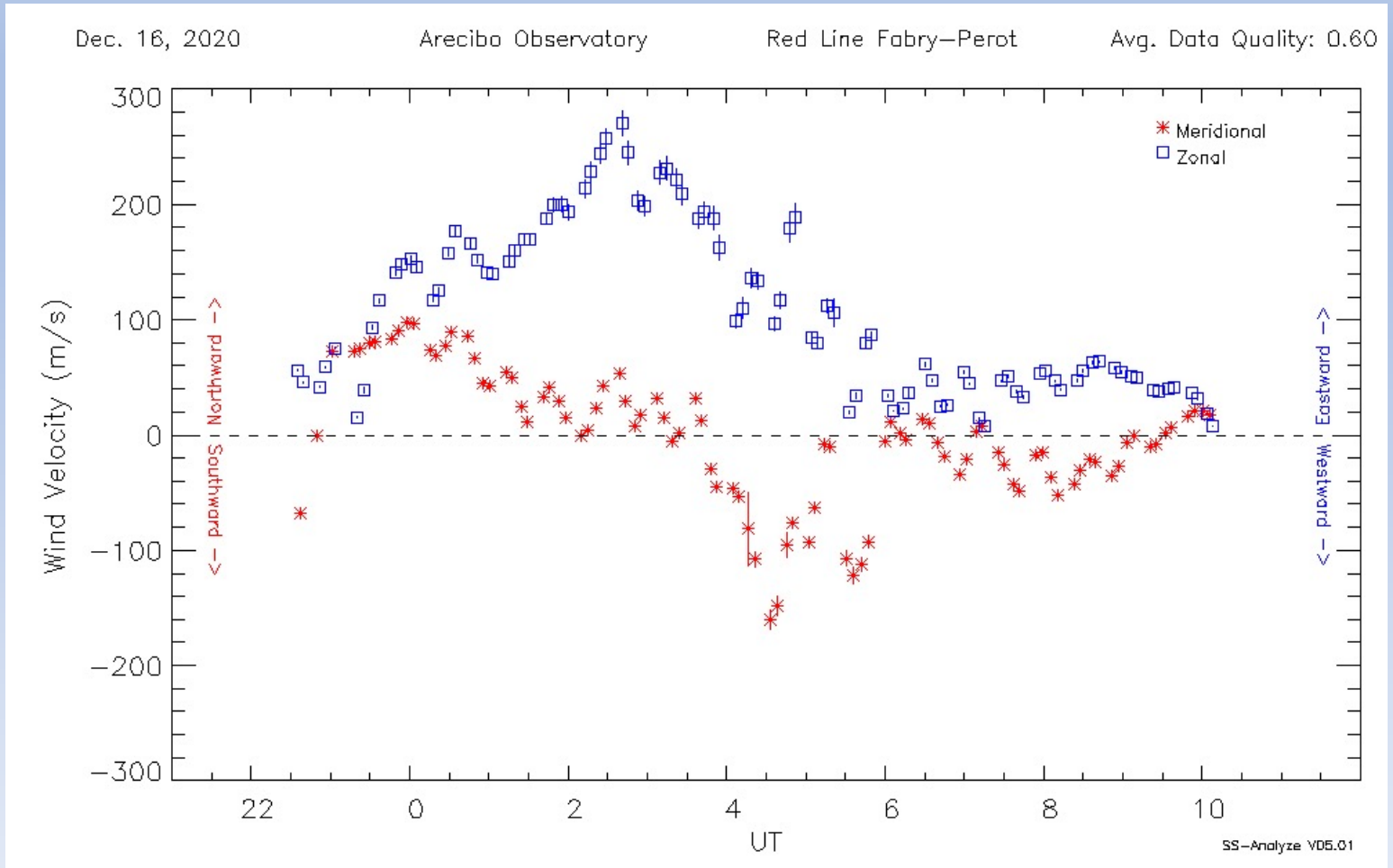

Derived meridional and zonal winds from Arecibo during the night beginning December 16, 2020; !5 days after the Gordon Telescope collapse.

Simultaneity

- Linear interpolations between data points are used to match the ICON measurement time stamps
- Average time between ICON & AO data time stamps = 8.2m merid., 8.4m, zonal
- Maximum time between ICON & AO time stamps = 66.0 merid. , 46.6m zonal

The outcome

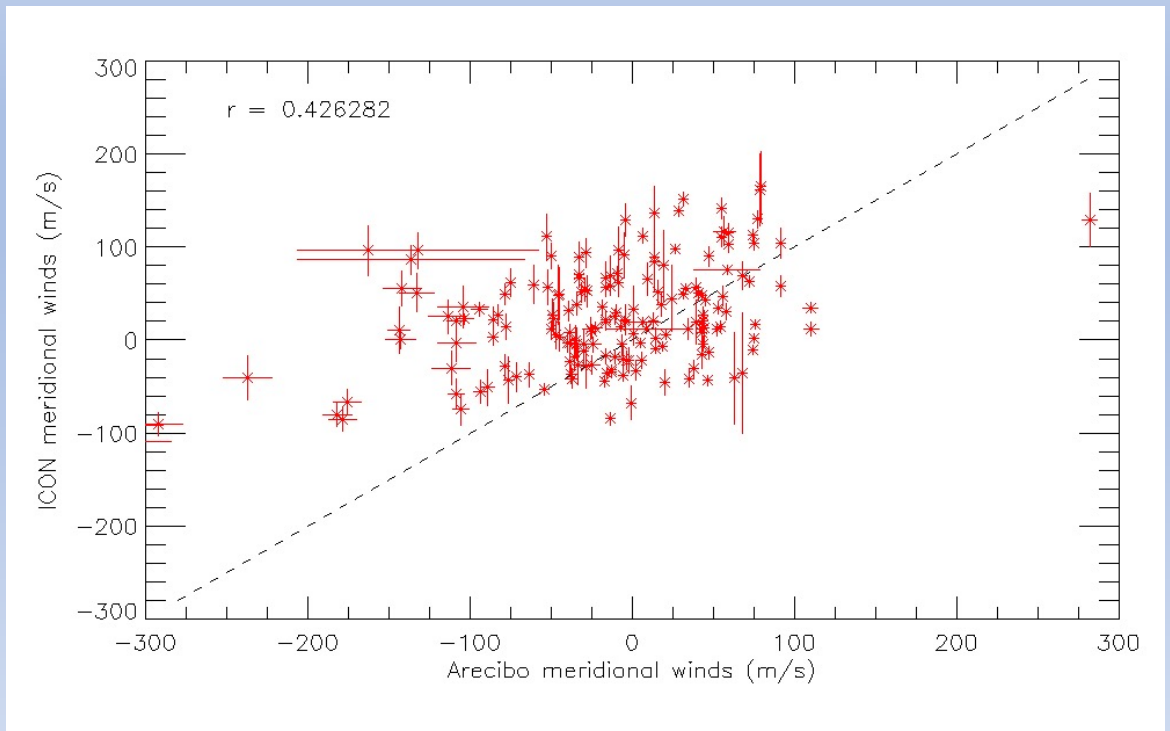

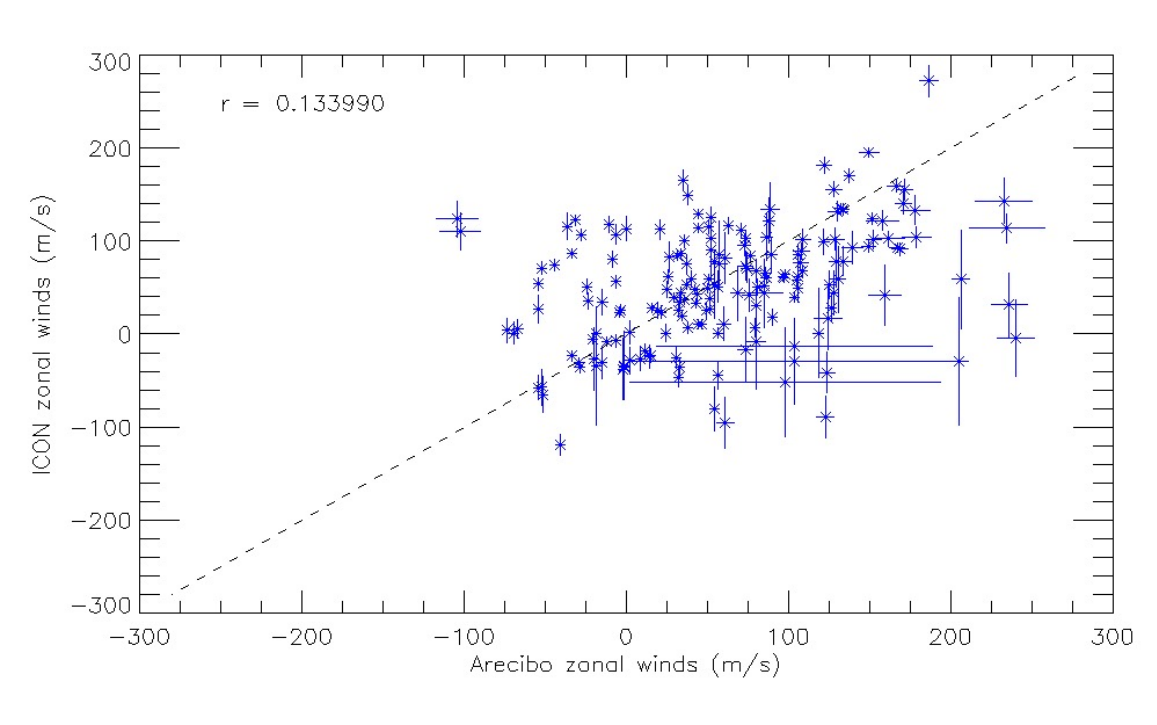

The Pearson correlation coefficient value, r, is quantified in the top left of each panel.
The dashed line is the r = 1 condition.

Comparison of Arecibo and ICON Wind vector measurements in 2020

ICON lat/long ±5° X ±5° from AO. No AO error constraint

Number of nighttime Overpasses by ICON in calendar year 2020:				359
Number of overlapping wind measurements:				183
Avg. time separation between AO/ICON time stamps (m):	meridional:	8.2	zonal:	8.4
Max. time separation between AO/ICON time stamps (m):	meridional:	66.0	zonal:	46.6

Median meridional wind error (m/s):	Arecibo:	1.0	ICON:	11.2
Median zonal wind error (m/s):	Arecibo:	1.9	ICON:	10.3
Pearson correlation coefficient:	meridional:	0.43	zonal:	0.13
AO/ICON vector pairs without error bar overlap:	meridional:	161 (88%)	zonal:	146 (80%)
AO/ICON vector pairs with opposite sign:	meridional:	74 (40%)	zonal:	44 (24%)
Average difference between AO and ICON vectors (m/s)	meridional:	75.5	zonal:	73.4

ICON lat/long ± 5° X ± 5° from AO. AO error < 5 m/s

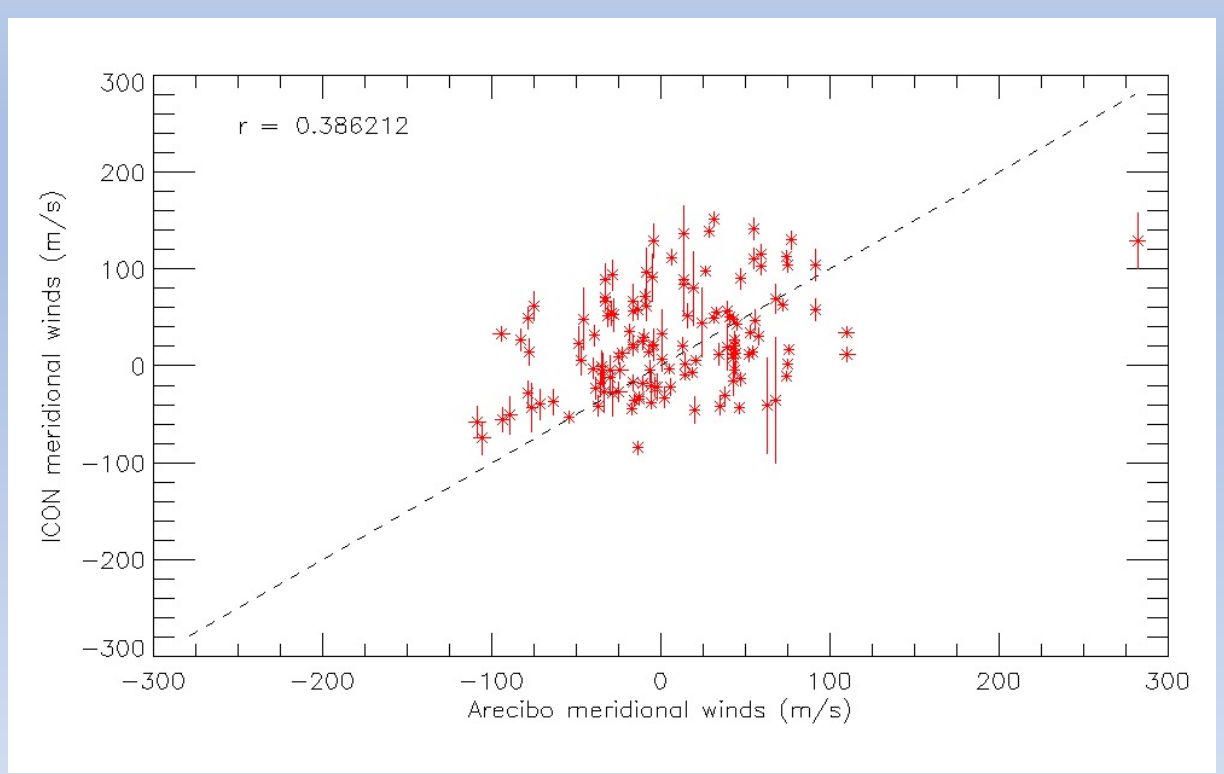

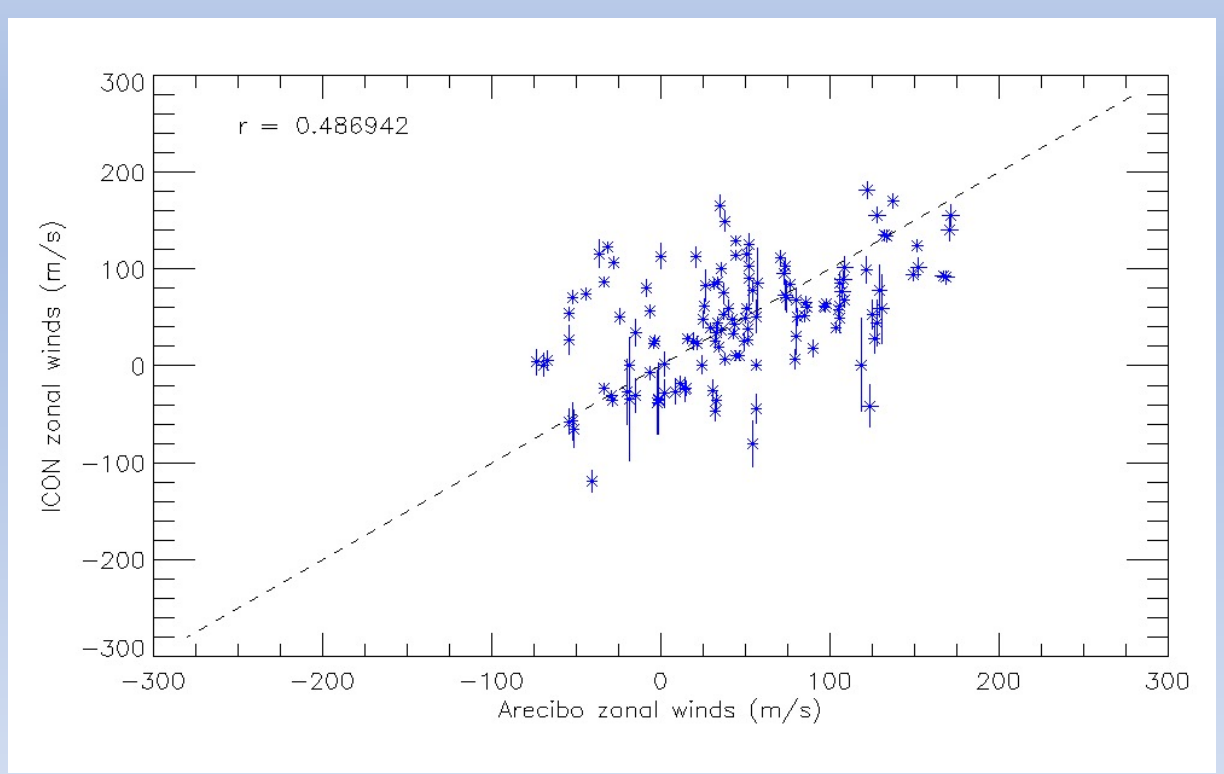

Number of nighttime Overpasses by ICON in calendar year 2020:				359
Number of overlapping wind measurements:				133
Avg. time separation between AO/ICON time stamps (m):	meridional:	6.5	zonal:	6.9
Max. time separation between AO/ICON time stamps (m):	meridional:	49.0	zonal:	46.6

Median meridional wind error (m/s):	Arecibo:	0.7	ICON:	9.4
Median zonal wind error (m/s):	Arecibo:	1.3	ICON:	7.2
Pearson correlation coefficient:	meridional:	0.39	zonal:	0.49
AO/ICON vector pairs without error bar overlap:	meridional:	115 (86%)	zonal:	106 (80%)
AO/ICON vector pairs with opposite sign:	meridional:	49 (37%)	zonal:	29 (22%)
Average difference between AO and ICON vectors (m/s)	meridional:	48.8	zonal:	45.2

ICON lat/long ±2.5° X ±2.5° from AO. No AO error constraint

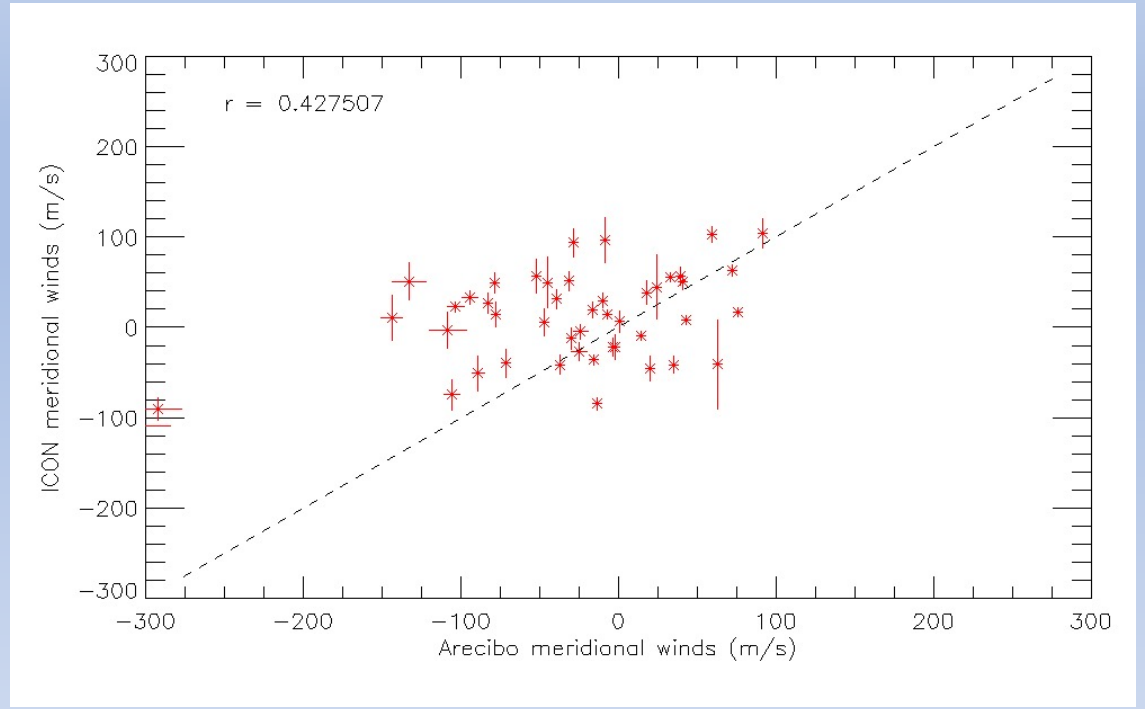

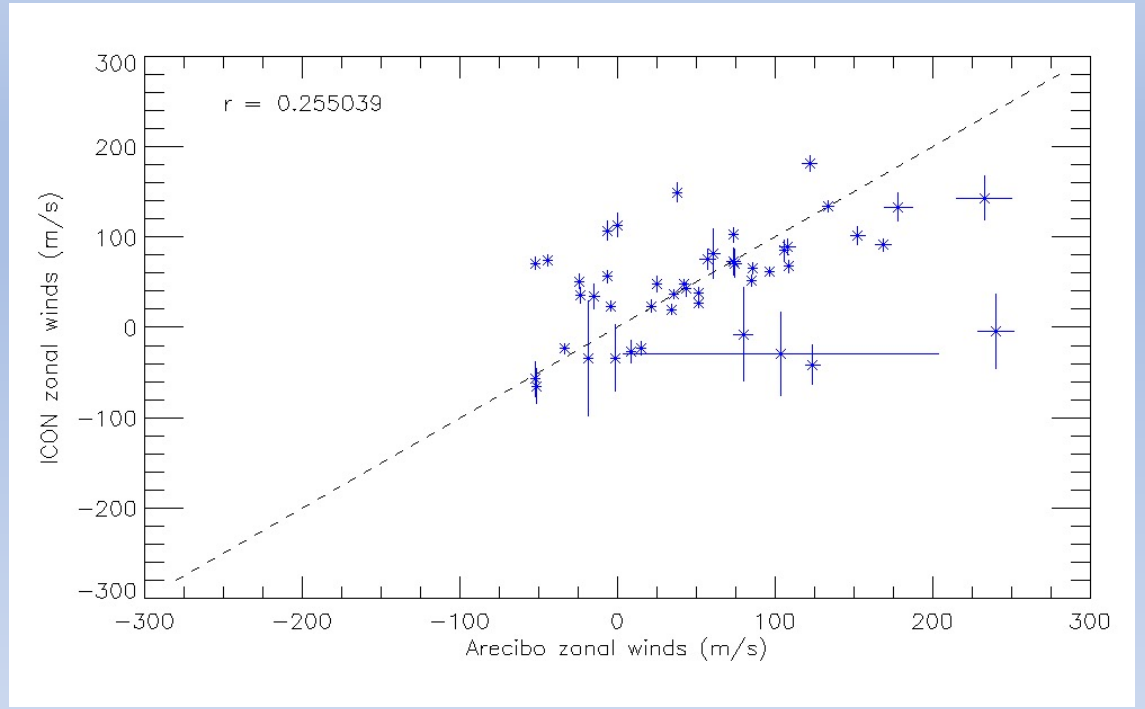

Number of nighttime Overpasses by ICON in calendar year 2020:				95
Number of overlapping wind measurements:				48
Avg. time separation between AO/ICON time stamps (m):	meridional:	6.8	zonal:	7.3
Max. time separation between AO/ICON time stamps (m):	meridional:	21.9	zonal:	25.9

Median meridional wind error (m/s):	Arecibo:	1.2	ICON:	11.6
Median zonal wind error (m/s):	Arecibo:	2.0	ICON:	8.7
Pearson correlation coefficient:	meridional:	0.43	zonal:	0.26
AO/ICON vector pairs without error bar overlap:	meridional:	42 (88%)	zonal:	36 (75%)
AO/ICON vector pairs with opposite sign:	meridional:	21 (44%)	zonal:	14 (29%)
Average difference between AO and ICON vectors (m/s)	meridional:	86.5	zonal:	69.7

ICON lat/long ±2.5° X ±2.5° from AO. AO error <5 m/s

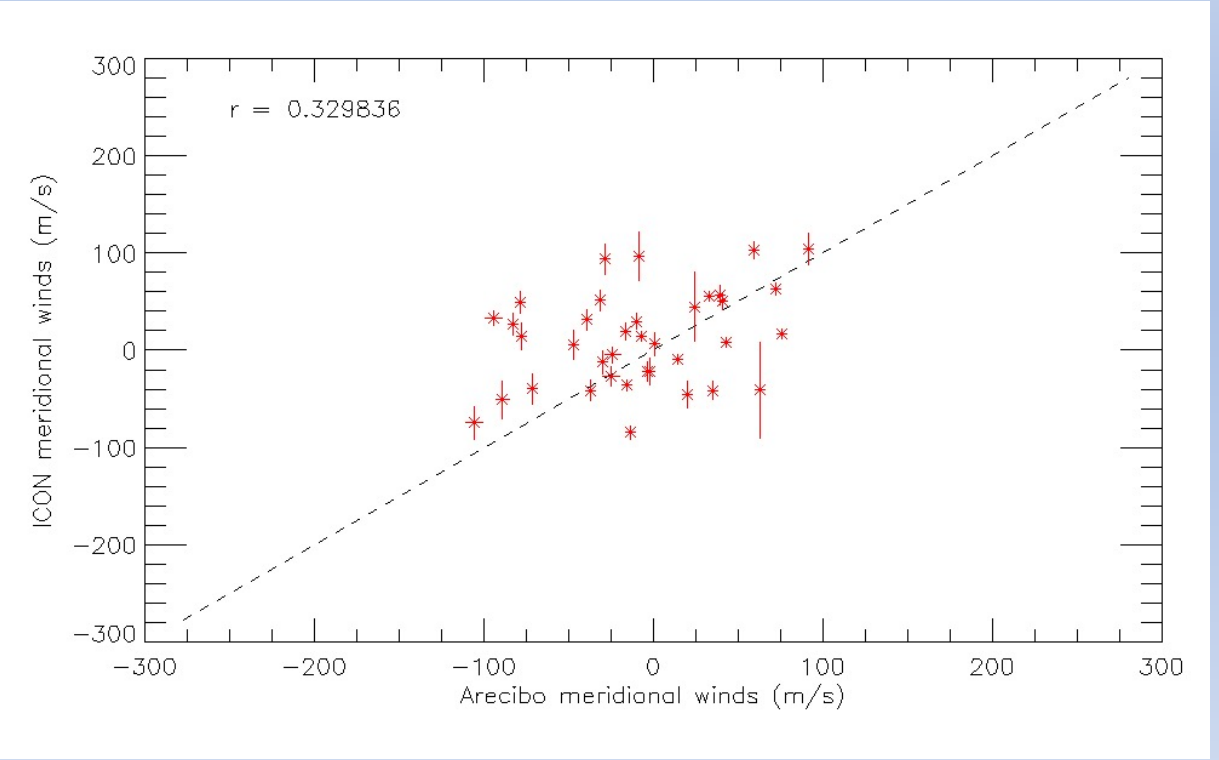

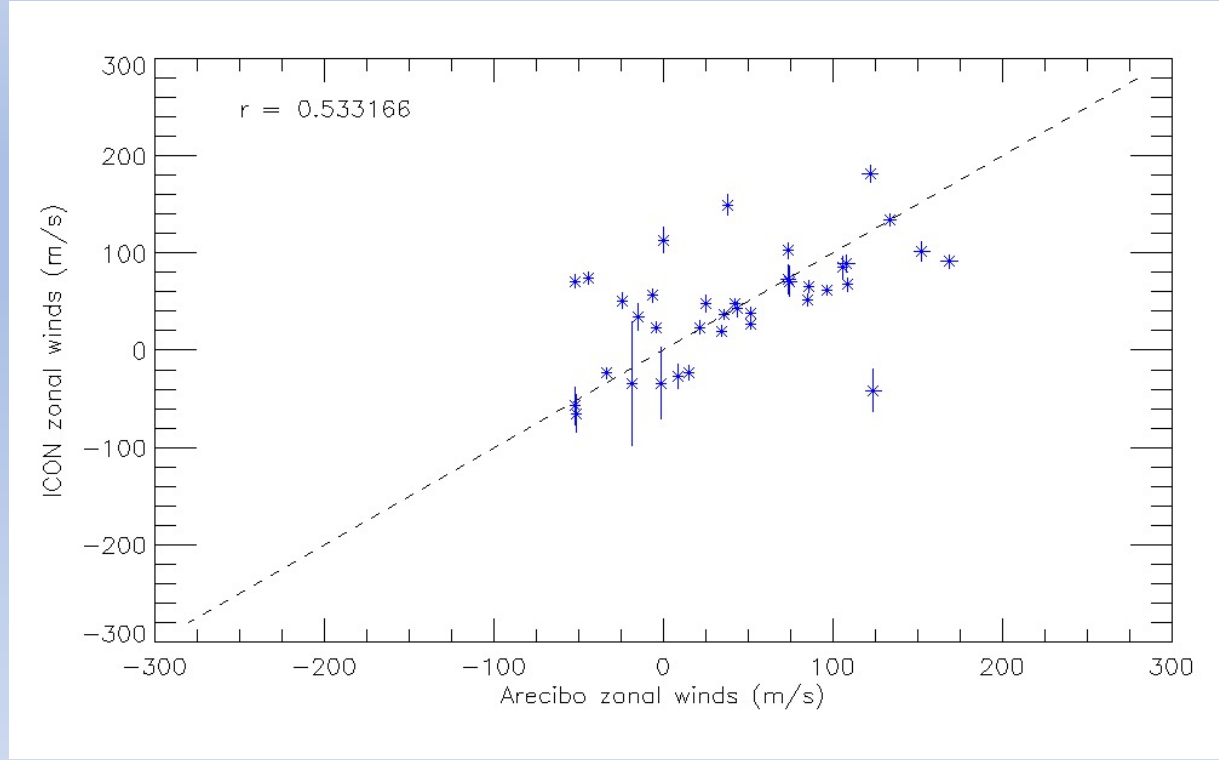

Number of nighttime Overpasses by ICON in calendar year 2020:				95
Number of overlapping wind measurements:				37
Avg. time separation between AO/ICON time stamps (m):	meridional:	6.4	zonal:	7.1
Max. time separation between AO/ICON time stamps (m):	meridional:	21.9	zonal:	25.9

Median meridional wind error (m/s):	Arecibo:	1.0	ICON:	10.4
Median zonal wind error (m/s):	Arecibo:	1.6	ICON:	7.9
Pearson correlation coefficient:	meridional:	0.33	zonal:	0.53
AO/ICON vector pairs without error bar overlap:	meridional:	31 (84%)	zonal:	27 (73%)
AO/ICON vector pairs with opposite sign:	meridional:	16 (43%)	zonal:	9 (24%)
Average difference between AO and ICON vectors (m/s)	meridional:	47.7	zonal:	39.8

ICON lat/long ± 5° X ± 5° from MH. No MH error limit

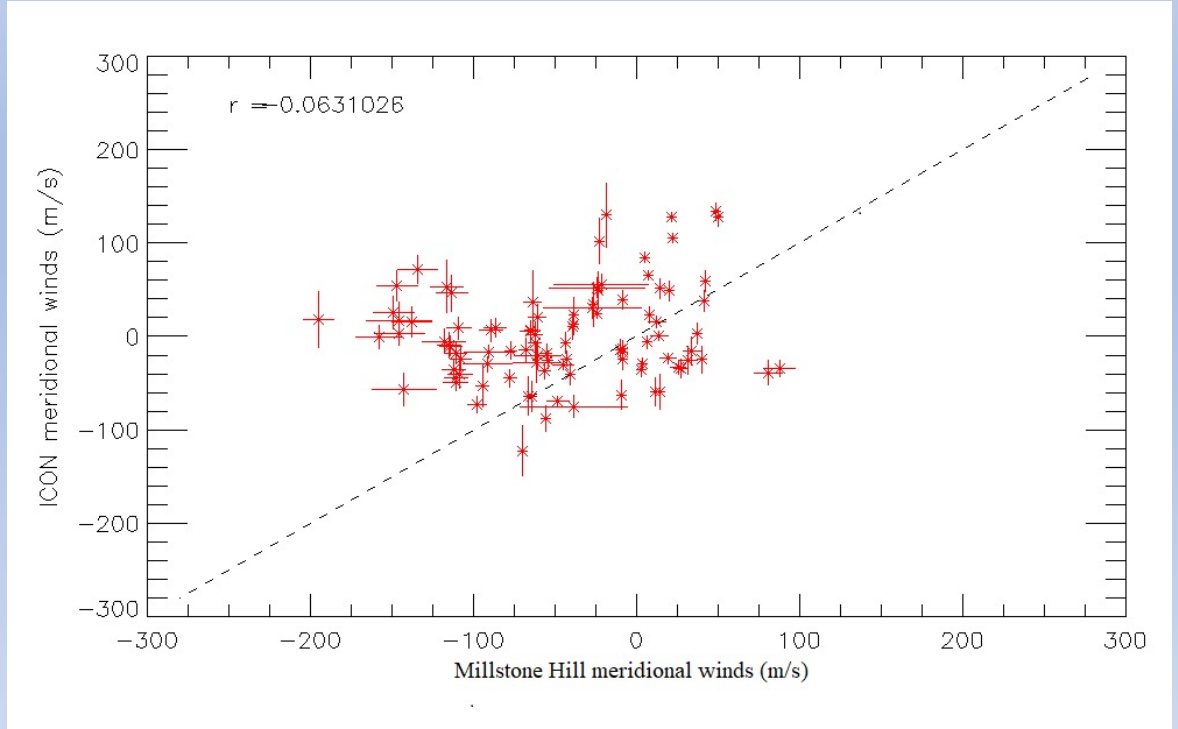

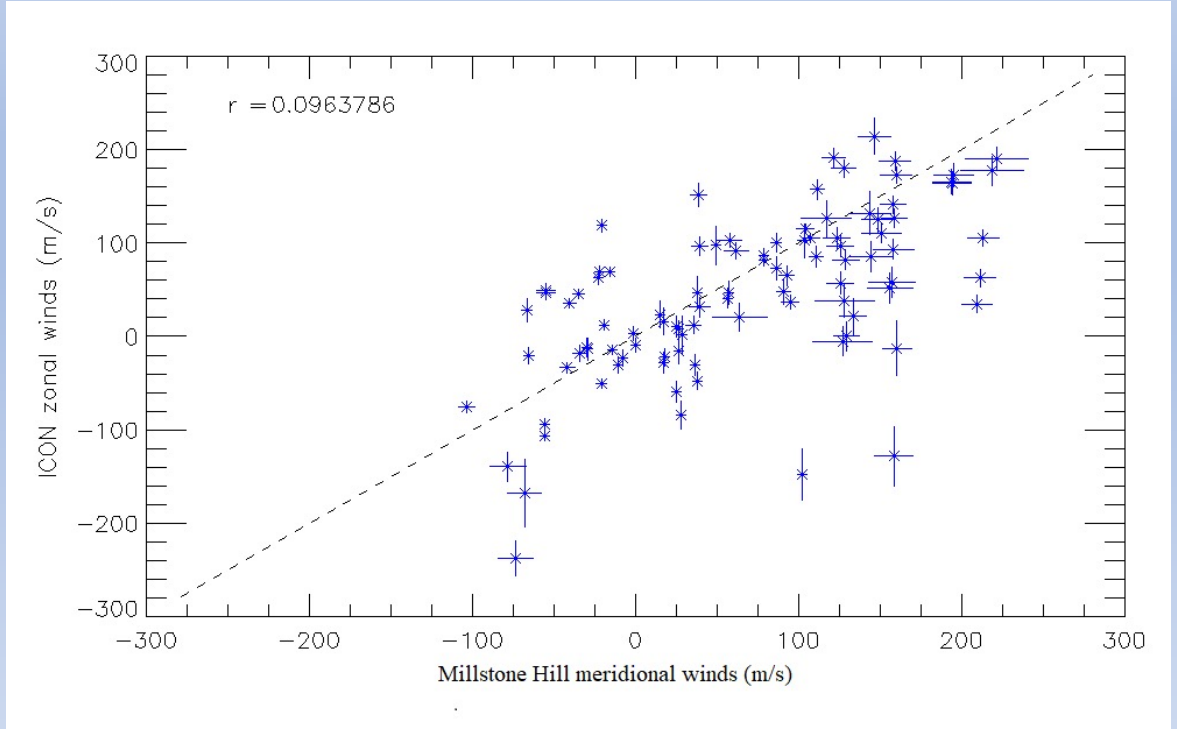

Number of nighttime Overpasses by ICON in calendar year 2020:				472
Number of overlapping wind measurements:				100
Avg. time separation between MH/ICON time stamps (m):	meridional:	15.0	zonal:	14.7
Max. time separation between MH/ICON time stamps (m):	meridional:	114.3	zonal:	107.1

Median meridional wind error (m/s):	Millstone:	4.2	ICON:	11.3
Median zonal wind error (m/s):	Millstone:	4.8	ICON:	10.8
Pearson correlation coefficient:	meridional:	-0.06	zonal:	0.10
MH/ICON vector pairs without error bar overlap:	meridional:	90 (90%)	zonal:	80 (80%)
MH/ICON vector pairs with opposite sign:	meridional:	45 (45%)	zonal:	25 (25%)
Average difference between MH and ICON vectors (m/s)	meridional:	81.7	zonal:	76.2

ICON lat/long ± 5° X ± 5° from MH. MH error limit <5m/s

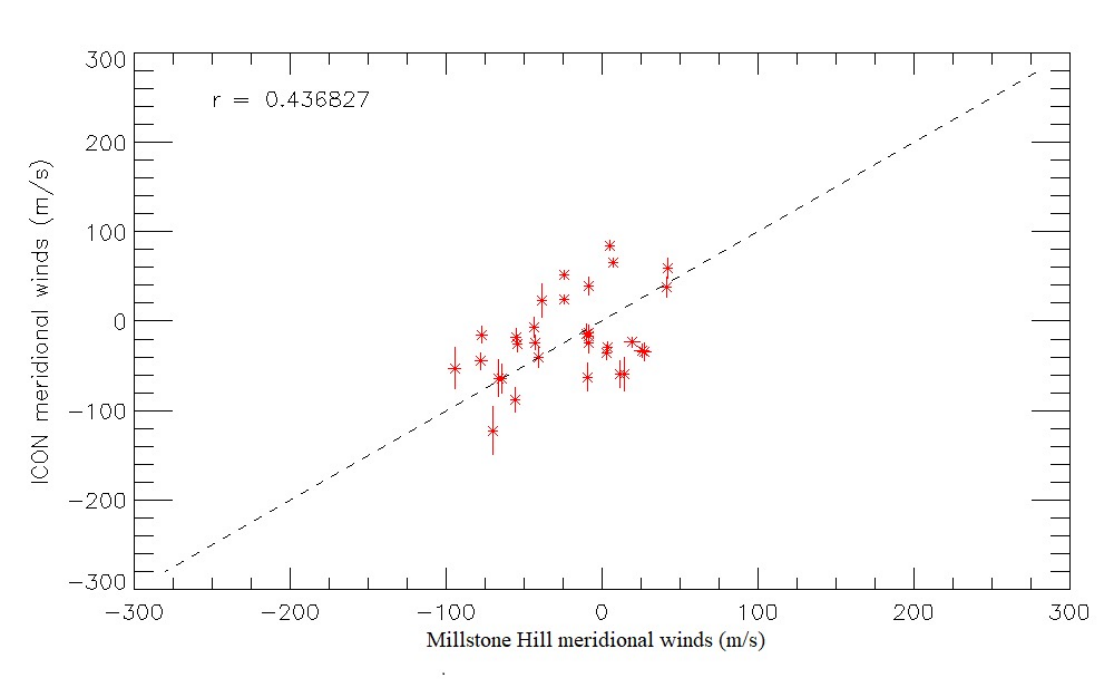

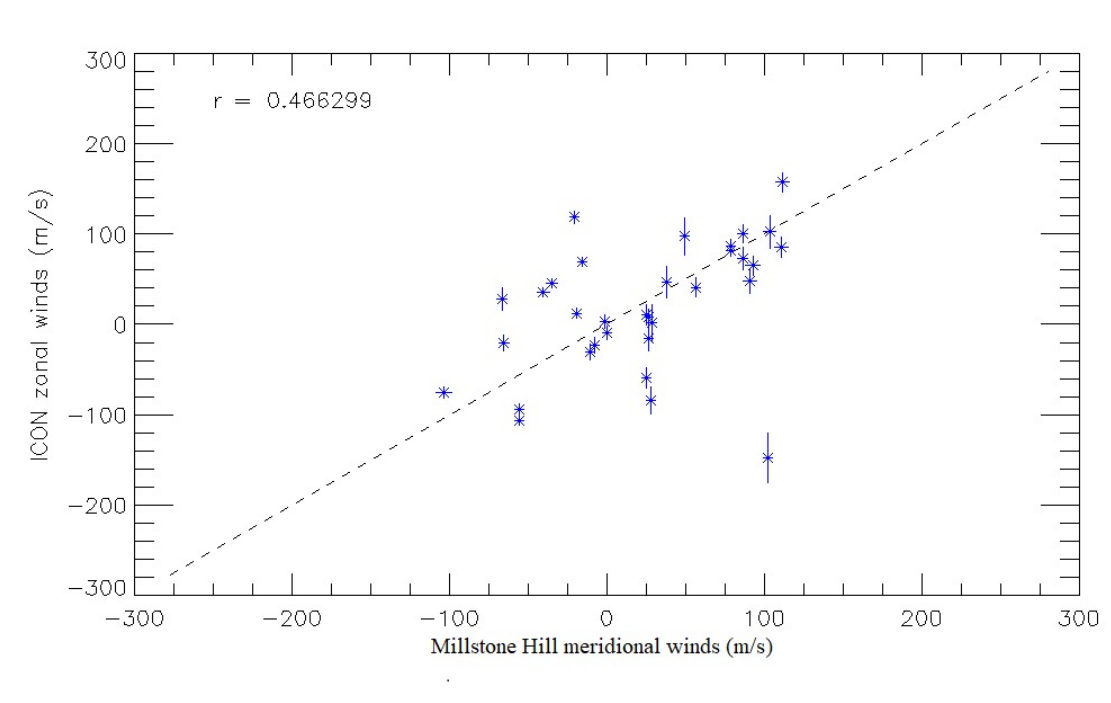

Number of nighttime Overpasses by ICON in calendar year 2020:				472
Number of overlapping wind measurements:				33
Avg. time separation between MH/ICON time stamps (m):	meridional:	7.0	zonal:	7.9
Max. time separation between MH/ICON time stamps (m):	meridional:	79.4	zonal:	94.4

Median meridional wind error (m/s):	Millstone:	1.6	ICON:	10.4
Median zonal wind error (m/s):	Millstone:	2.2	ICON:	9.8
Pearson correlation coefficient:	meridional:	0.44	zonal:	0.47
MH/ICON vector pairs without error bar overlap:	meridional:	26 (79%)	zonal:	27 (82%)
MH/ICON vector pairs with opposite sign:	meridional:	11 (33%)	zonal:	12 (36%)
Average difference between MH and ICON vectors (m/s)	meridional:	36.6	zonal:	46.1

Initial attempts to constrain the Arecibo and Millstone Hill comparisons with ICON data do not reconcile our results with those of *Makela et al.*, 2020.

Makela et al. 2020 compared the ICON vectors to data from the FPI at the Urbana Atmospheric Observatory (UAO) and found r=0.88 for both meridional and zonal wind comparisons.

	AO ±5° X ±5°	±5° X ±5° AO error < 5 m/s	AO ±2.5° X ±2.5°	±2.5° X ±2.5° AO error < 5 m/s	MH ±5° X ±5°	±5° X ±5° MH error < 5 m/s
# of overlap	183	133	48	37	100	33
Median meridional error, AO (m/s)	1.0	0.9	1.2	1.0	4.2	1.6
Median meridional error, ICON (m/s)	11.2	10.2	11.6	10.4	11.3	10.4
Median zonal error, AO (m/s)	1.9	1.3	2.0	1.6	4.8	2.2
Median zonal error, ICON (m/s)	10.3	8.4	8.7	7.9	10.8	9.8
Average difference meridional, (m/s)	75.5	48.8	86.5	47.7	81.7	36.6
Average difference zonal, (m/s)	73.4	45.2	69.7	39.8	76.2	36.1
No error bar overlap merid.	88%	86%	88%	84%	90%	79%
No error bar overlap zonal	80%	80%	75%	73%	80%	82%
Opposite directions merid.	44%	37%	44%	43%	45%	33%
Opposite directions zonal	24%	22%	29%	24%	25%	36%
Correlation coefficient r meridional	0.43	0.39	0.44	0.33	-0.06	0.44
Correlation coefficient r zonal	0.13	0.49	0.26	0.53	0.10	0.47

Summary

We hypothesize:

This analysis is improperly biased, or the Arecibo & Millstone Hill data or analyses are systematically flawed.

Some ideas for future re-analysis work:

- smaller Lat/Long bins defining an ICON overflight of Arecibo
- Further constrain data selection with only the “best” associated statistical wind errors
- Reduce the allowed time difference between the ICON time stamps and AO data time stamps
- Repeat the analysis as functions of season or month (to minimize MIGHTI drift impact)
- Try selecting all ICON wind vectors from the same altitude
- Upcoming MIGHTI data updates, (version 5.0) may include drift and error bar corrections

References

Englert, C.R., M.H. Stevens, D.E. Siskind, J.M. Harlander, F.L. Roesler, H.M. Pickett, C. von Savigny and A. J. Kochenash, First results from the Spatial Heterodyne Imager for MesosphericRadicals (SHIMMER): Diurnal variation of mesospheric hydroxyl, (2008), *Geophys. Res. Lett, 35*, L19,813 – L19,8, doi:10.1029/2008GL035420.

Englert, C.R., M.H. Stevens, D.E. Siskind, J.M. Harlander and F. L. Roesler, Spatial Heterodyne Imager for Mesospheric Radicals on STPSat-1, (2010), *J. Geophys. Res., 115*, D20306, doi:10.1029/2010JD014398.

Englert, C.R., J.M.Harlander, C.M.Brown, J.W.Meriwether, J.J.Makela, M.Castelaz, J.T.Emmert, D.P.Drob, K.D.Marr, Coincident thermospheric wind measurements using ground-based Doppler Asymmetric Spatial Heterodyne (DASH) and Fabry–Perot Interferometer (FPI) instruments, (2012), J. Atmos. And *Solar-Terr Phys., 86*, 92-98, doi:/10.1016/j.jastp.2012.07.002.

Harding, B.J., J.J. Makela, C.R. Englert, K.D. Marr, J.M. Harlander, S.L. England, T.J. Immel, The MIGHTIWind Retrieval Algorithm: Description and Verification, (2017), *Space Sci Rev, 212*, 585–600 doi:10.1007/s11214-017-0359-3.

Harlander, J.M., F.L. Roesler, C. R. Englert, J.G. Cardon, R.R. Conway, C.M. Brown and J. Wimperis, Robust monolithic ultraviolet interferometer for the SHIMMER instrument on STPSat-1, (2003), *App. Optics 42(15)*, 2829-2834, doi:/10.1364/AO.42.002829.

J.M. Harlander, J.E. Lawler, J. Corliss, F.L. Roesler and W.M. Harris, First results from an all-reflection spatial heterodyne spectrometer with broad spectral coverage, (2010), *Optics Express 18(6)*, 6205-6210, doi:/10.1364/OE.18.006205.

Makela, J.J., M. Baughman, L.A. Navarro, B.J. Harding, C.R. Englert , J.M. Harlander, K.D. Marr, Z. Benkhaldoun, M. Kaab and T.J. Immel, Validation of ICON-MIGHTI Thermospheric Wind Observations: 1. Nighttime Red-Line Ground-Based Fabry-Perot Interferometers, (2020), *J. Geophys. Res., 126*. doi: /10.1029/2020JA028726.

Shepherd, G.G., G. Thuillier, W. A. Gault, B. H. Solheim, C. Hersom, J. M. Alunni, J.-F. Brun, S. Brune, P. Charlot, L. L. Cogger, D.-L. Desaulniers, W. F. J. Evans, R. L. Gattinger, F. Girod, D. Harvie, R. H. Hum, D. J. W. Kendall, E. J. Llewellyn, R. P. Lowe, J. Ohrt, F. Pasternak, O. Peillet, I. Powell, Y. Rochon, W. E. Ward, R. H. Wiens, and J. Wimperis, WINDII, the wind imaging interferometer on the Upper Atmosphere Research Satellite, (1993), *J. Geophys Res., 98(D6)*, 10,7250 – 10,750, 1993. doi.org/10.1029/93JD00227.